



ELSEVIER

Available online at www.sciencedirect.com ScienceDirect

Proceedings of the Combustion Institute 31 (2007) 1691–1699

**Proceedings
of the
Combustion
Institute**

www.elsevier.com/locate/proci

Modeling of filtered heat release for large eddy simulation of compressible infinitely fast reacting flows

Juan Pedro Mellado ^{a,*}, Rainer Friedrich ^a, Sutanu Sarkar ^b^a *Fachgebiet Stroemungsmechanik, Technische Universitaet Muenchen, Boltzmannstr. 15, D-85748 Garching, Germany*^b *Department of Mechanical and Aerospace Engineering, University of California San Diego, La Jolla, CA 92093-0411, USA*

Abstract

A priori and *a posteriori* studies for large eddy simulation of the compressible turbulent infinitely fast reacting shear layer are presented. The filtered heat release appearing in the energy equation is unclosed and the accuracy of different models for the filtered scalar dissipation rate and the conditional filtered scalar dissipation rate of the mixture fraction in closing this term is analyzed. The effect of different closures of the subgrid transport of momentum, energy and scalars on the modeling of the filtered heat release via the resolved fields is also considered. Three explicit models of these subgrid fluxes are explored, each with an increasing level of reconstruction and all of them regularized by a Smagorinsky-type term. It is observed that a major part of the error in the prediction of the conditional filtered scalar dissipation comes from the unsatisfactory modeling of the filtered dissipation itself. The error can be substantial in the turbulent fluctuation (rms) of the dissipation fields. It is encouraging that all models give good predictions of the mean and rms density in *a posteriori* LES of this flow with realistic heat release corresponding to large density change. Although *a posteriori* results show a small sensitivity to subgrid modeling errors in the current problem, extinction–reignition phenomena involving finite-rate chemistry would demand more accurate modeling of the dissipation rates. *A posteriori* results also show that the resolved fields obtained with the approximate reconstruction using moments (ARM) agree better with the filtered direct numerical simulation since the level of reconstruction in the modeled subfilter fluxes is increased.

© 2006 The Combustion Institute. Published by Elsevier Inc. All rights reserved.

Keywords: Large eddy simulation; Compressible; Dissipation; Infinitely fast

1. Introduction

The mixing process of scalars is of primary importance in turbulent non-premixed combustion, since it determines how fast the reactants can react, or even if the reaction can progress at all [1]. In LES, for filter sizes and Reynolds num-

bers of technical interest, the mixing process occurs mainly in the subfilter range of scales and it has to be modeled [2]. The two related quantities required in LES of non-premixed turbulent combustion are the filtered scalar dissipation rate $\bar{\chi}$ and the filtered scalar dissipation rate conditioned on the scalars Z present in the problem, $\bar{\chi}_Z$.

A priori model analysis of such quantities has been reported by several authors [2–4]. *A posteriori* results, using an incompressible formulation, have been reported for the case of infinitely fast

* Corresponding author. Fax: +49 89 289 16139.
E-mail address: mellado@gmx.de (J.P. Mellado).

chemistry [5] as well as for the case of finite rate chemistry [6,7]. The general conclusion is that the dissipation models for \tilde{X} are good enough for those particular reacting flows because there is a small sensitivity of the LES to them, although sometimes the prediction of statistics of \tilde{X} itself is quite erroneous [6]. However, when extinction–reignition phenomena are present, those same errors in the statistics of the modeled \tilde{X} or \tilde{X}_Z may lead to substantial inaccuracies.

Further study of the scalar dissipation models required in LES of turbulent combustion is here presented. Modeling of \tilde{X} and the effect of different resolved fields on it are first addressed. Next, \tilde{X}_Z is investigated. \tilde{X}_Z is normally obtained from \tilde{X} , the filtered or large-scale distribution function of Z , and some additional hypothesis. Thus, it is desired to know how much of the error in \tilde{X}_Z is due to this last step and how much of it stems from the model of \tilde{X} .

For this purpose, a compressible LES formulation of the infinitely fast chemistry case is chosen (i.e., the density is *not* computed from the mixture fraction Z , but the energy equation is retained). *A posteriori* results of the incompressible case have already been reported [8,9], but the dissipation rates do not enter in such an incompressible description. In the compressible shear layer LES of Menon et al. [10], the dissipation rate does not enter because subgrid mixing is accomplished with the linear eddy model. With the present compressible formulation, the conditional dissipation rate \tilde{X}_Z at the stoichiometric surface appears as one of the main terms in the energy equation, through the filtered heat release. The simplification of the chemistry allows to assess the performance of the different dissipation models better than when more detailed chemistry is considered, because this latter case introduces more uncertainties. In addition, DNS at realistic Reynolds numbers is more feasible here than when finite rate chemistry is retained, which leads to more precise and controlled comparisons than with experiments. Note that knowledge of \tilde{X}_Z is necessary not only for LES based on infinitely fast chemistry but also for that based on the flamelet approximation, conditional moment closure or transported density function methods.

The DNS by Pantano et al. [11] of the compressible temporally evolving shear layer studying

the Burke–Schumann limit of methane–air combustion with realistic heat release effect (density variation of 7:1) is taken as reference. Only the fully turbulent stage is considered here. Three DNS flow fields at three different times are available. Using the first of them as time origin, $\tau_1 = 0$, the other two correspond to non-dimensional times $\tau = t\Delta U/\delta_{\omega,1}$ of $\tau_2 = 4.0$ and $\tau_3 = 17.4$, ΔU being the velocity difference of the shear layer and $\delta_{\omega,1}$ the vorticity thickness at τ_1 . The vorticity thickness increases with time up to $\delta_{\omega,2} = 1.21\delta_{\omega,1}$ and $\delta_{\omega,3} = 1.69\delta_{\omega,1}$, respectively. The Reynolds number $Re_{\omega} = \rho_0\Delta U\delta_{\omega}/\mu$ at τ_3 is $Re_{\omega,3} = 1.4 \times 10^4$, the stoichiometric mixture fraction $Z_s = 0.2$, and the convective Mach number 0.3.

The local instantaneous scalar dissipation rate is $X = 2D_Z|\nabla Z|^2$, including the mean and the turbulent fluctuation. The molecular diffusion coefficient of the mixture fraction Z is D_Z . Given a field ϕ , filtering is denoted as $\tilde{\phi}$ and Favre (density weighted) filtering as $\tilde{\phi}$. Averages are calculated as plane averages and indicated by $\langle \phi \rangle$, Favre averages by $\langle \phi \rangle^f$.

After briefly describing the filters, the models for the subgrid transport and the heat release terms are discussed, presenting *a priori* results when required. We conclude with the *a posteriori* section.

2. Filter

A top-hat filter based on the midpoint rule is employed. Two filter sizes are considered, $\Delta_f = 4\Delta_g$ and $\Delta_f = 8\Delta_g$, where Δ_g is the original DNS grid spacing. Finally, the fields are sampled onto the LES grid with spacing $\Delta_f/2$.

Table 1 shows α , the amount of subfilter variance, $(Z^2)_{\text{sg}} = \tilde{Z}^2 - \tilde{Z}^2$, relative to the total fluctuation, Z_{rms}^2 . This parameter α , the subfilter content of the scalar fluctuations, varies between 10% and 40% here. The decrease of α with time is consistent with the increase of the Kolmogorov scale with time. On the other hand, α grows as the filter becomes stronger. The parameter β in Table 1, to be discussed later, denotes the subgrid fraction of the scalar dissipation.

Table 1

Ratio $\alpha = \int \langle \tilde{\rho}(Z^2)_{\text{sg}} \rangle dy / \int \langle \tilde{\rho} \rangle Z_{\text{rms}}^2 dy$ and $\beta = \int \langle \tilde{\rho} X^{\text{sg}} \rangle dy / \int \langle \tilde{\rho} \tilde{X} \rangle dy$ for different filters F_i and times τ_i

	Δ_f/Δ_g	α			β		
		τ_1	τ_2	τ_3	τ_1	τ_2	τ_3
F_1	4	0.14	0.12	0.10	0.49	0.49	0.46
F_2	8	0.38	0.33	0.28	0.78	0.79	0.74

3. Subgrid transport model

Models are required for the subgrid contribution to the transport by the velocity u of quantities ζ per unit volume, e.g., ρu , ρ and ρZ , the *subfilter flux*

$$q_\zeta = \overline{\zeta(\rho u)} / \bar{\rho} - \bar{\zeta} \overline{(\rho u)} / \bar{\rho}. \quad (1)$$

Reconstruction approaches [12], like the scale similarity model [13] or the deconvolution model [14], use *intermediate fields* ζ^m to close these subgrid fluxes. However, they need regularization to achieve stability. A Smagorinsky-like term is utilized here

$$q_\zeta^m = \overline{\zeta^m(\rho u)^m} / \bar{\rho} - \overline{\zeta^m(\rho u)^m} / \bar{\rho} - \bar{\rho} D_\zeta^{\text{smg}} [\nabla(\bar{\zeta} / \bar{\rho})]^{\text{sa}}, \quad (2)$$

where $[\cdot]^{\text{sa}}$ indicates the symmetric anisotropic part when ζ is the momentum.

Three cases are considered: (1) no reconstruction term, which is the standard dynamic Smagorinsky model and denoted by SMG, (2) the scale similarity model for the reconstruction term, which would be the standard dynamic mixed model and denoted by SSM, and (3) the approximate reconstruction by moments model for the reconstruction term, referred as ARM. The Smagorinsky constant is determined dynamically [15], the test filter being a top-hat filter of size $2\Delta_f$. Only the turbulent fluctuation fields are considered for the modeling of the subgrid fluxes [16].

In the ARM case, the intermediate field is constructed by

$$\zeta^m = \bar{\zeta} + c_{\zeta,0} (\bar{\zeta} - \bar{\zeta}), \quad (3)$$

where the model coefficients $c_{\zeta,0}$ are computed so that the average subgrid scalar variance agrees between the exact field and the intermediate field. A comprehensive discussion of the formulation for general non-linear functions of a scalar can be found in [12], extending the method here to the velocity and pressure fields. The model coefficient is obtained from a quadratic equation (cf. Eqs. (23) and (24) in [12]), where the total variance of the turbulent field has to be provided. Instead of a spectral formulation, one based on integral quantities across the shear layer is adopted here. For instance, in the case of the scalar, $\int \langle \rho \rangle Z_{\text{rms}}^2 dy$ is calculated from the DNS at the three available times and a linear fit provides the required integral quantity during the LES.

The three explicit models SMG, SSM and ARM, postulate, in this order, an increasing amount of subgrid transport that is represented by the reconstruction part. No implicit filtering is considered.

4. Subgrid reaction model

The energy equation is formulated in terms of the pressure. Taking the specific heat ratio, γ , to be constant under the filtering operation, the filtered heat release $\bar{\rho} \tilde{S}$ can be written exactly in the Burke–Schumann limit as

$$\bar{\rho} \tilde{S} = (\gamma - 1) Q_e \bar{\rho} \tilde{X}_s \tilde{P}_s, \quad (4)$$

where \tilde{X}_s is the conditional filtered dissipation rate $\tilde{X}_Z(Z')(x, t)$ and \tilde{P}_s is the Favre filtered density function $\tilde{P}_Z(Z')(x, t)$, both evaluated at the stoichiometric surface $Z' = Z_s$, and Q_e is an appropriate heat release parameter. Equation (4) is the LES equivalent to the Reynolds average expression derived by Bilger [17].

The whole term $\tilde{X}_s \tilde{P}_s$ requires modeling, although \tilde{X}_s and \tilde{P}_s are usually treated separately. Following common practice, \tilde{P}_Z is modeled by a beta distribution. This choice is supported by the following result: the correlation coefficients between the exact and the predicted fields of \tilde{Z}^3 and \tilde{Z}^4 , were calculated in the core region and they were over 0.99. The challenge is to model the scalar dissipation rates.

4.1. Filtered dissipation rate

The conditional filtered scalar dissipation rate is often related to the filtered scalar dissipation rate $\tilde{X}(x, t) = 2\bar{\rho} D_Z \nabla Z \cdot \nabla Z / \bar{\rho}$, which also needs modeling, common practice [6,5,7] being

$$\tilde{X}^m = X^r + X^{\text{sg}} \quad (5)$$

based on the concept of local equilibrium of scales at the filter size. $X^r = 2\bar{\rho} D_Z \nabla Z \cdot \nabla Z / \bar{\rho}$ is the resolved scalar dissipation rate, and $X^{\text{sg}} = -2q_Z \cdot \nabla Z / \bar{\rho}$ is the subgrid scalar dissipation rate. This approach can be justified, to some extent, from the transport equations of \tilde{Z}^2 and \tilde{Z}^2 , which provide the exact expression

$$\begin{aligned} \frac{d}{dt} \int \langle \bar{\rho} \rangle \langle (Z^2)_{\text{sg}} \rangle^f dy \\ = \int \langle \bar{\rho} \rangle \left(\langle X^r \rangle^f + \langle X^{\text{sg}} \rangle^f - \langle \tilde{X} \rangle^f \right) dy. \end{aligned} \quad (6)$$

Equation (6) shows that the model Eq. (5) for the filtered dissipation rate \tilde{X} has an error in the volume average value given by the temporal evolution of the total subgrid scalar variance. The DNS data show that this error is small, of the order of 5% of the filtered dissipation, and diminishing as α decreases.

Therefore, the field X^{sg} is of interest. Figure 1 shows the Favre average of X^{sg} as a function of the normalized crosswise coordinate y . The subgrid scalar dissipation depends on the filter, and increases appreciably as the filter becomes stronger. The SSM over-estimates the subgrid dissipa-

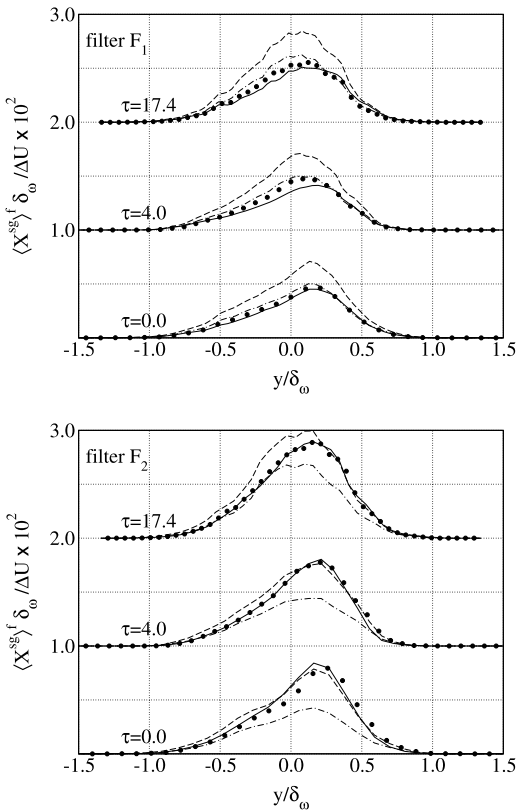


Fig. 1. Favre average of the subgrid scalar dissipation rate per unit mass: •, exact (filtered DNS); —, ARM model; --SSM model; -·-, SMG model. Times $\tau = 4.0$ and $\tau = 17.4$ have an offset in ordinates of 1.0 and 2.0, respectively.

tion, when the subfilter content α is small (filter F_1), SMG providing a better estimate. As α increases, the SMG tends to under-estimate the actual value and SSM reduces its error, so that, with the filter F_2 , SSM provides better mean subgrid dissipation than SMG, which under-estimates it by almost 50%. ARM provides the best performance, being filter-independent and accurate for a wide range of filter sizes.

The filtered dissipation rate \tilde{X}^m is then calculated by Eq. (5). The exact average subgrid dissipation was observed in Fig. 1 to increase with the filter size. In turn, the resolved dissipation diminishes, and the sum of both varies very little, according to Eq. (6). This behavior is given quantitatively by the parameter β in Table 1. The prediction of the average value given by the different models behaves similarly to that of the subgrid transfer, the relative error being reduced because the resolved dissipation rate now added is exact. The SMG under-prediction agrees with Ref. [6], which reports model values of $\langle \tilde{X}^m \rangle^f$ between 25–45% of the exact value, the error decreasing with decreasing α , as found here.

The root-mean-square (rms) of the turbulent fluctuation of X^{sg} and \tilde{X} are now considered. Too high values of \tilde{X}_{rms} are given by Eq. (5), as will be seen below, and the model

$$X^m = X^r + X^{sg}, \tag{7}$$

is found to be more appropriate because the additional filtering operation to obtain \tilde{X}^m reduces $(\tilde{X}^m)_{rms}$ with respect to model Eq. (5). Equation (7) leads also to the small mean error predicted by Eq. (6), because $\int \langle \rho Z^2 \rangle dy \approx \int \langle \tilde{\rho} \tilde{Z}^2 \rangle dy$, and Eq. (7) agrees better than Eq. (5) with the formulation proposed by Ref. [2], discussed later.

The rms of X^{sg} is shown in Fig. 2. For filter F_1 , with small energy content α , SSM over-estimates the actual fluctuation, the SMG under-estimates it, and ARM provides it better. For a stronger filter, case F_2 , SSM and ARM perform similarly well, but SMG clearly under-predicts the actual value by more than a factor of two.

The rms of \tilde{X} , shown in Fig. 3, behaves differently from that of the subgrid transfer, Fig. 2. Here, SSM clearly over-predicts the actual value,

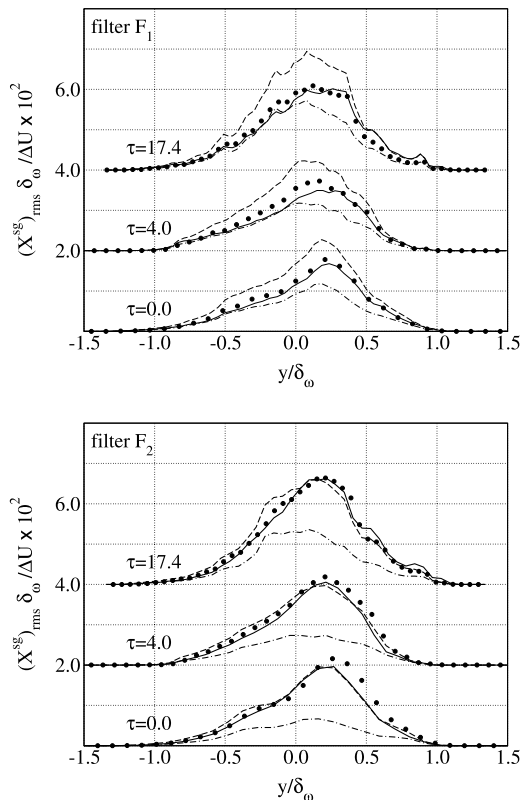


Fig. 2. Rms of the subgrid scalar dissipation rate per unit mass: •, exact (filtered DNS); —, ARM model; --, SSM model; -·-, SMG model. Times $\tau = 4.0$ and $\tau = 17.4$ have an offset in ordinates of 2.0 and 4.0, respectively.

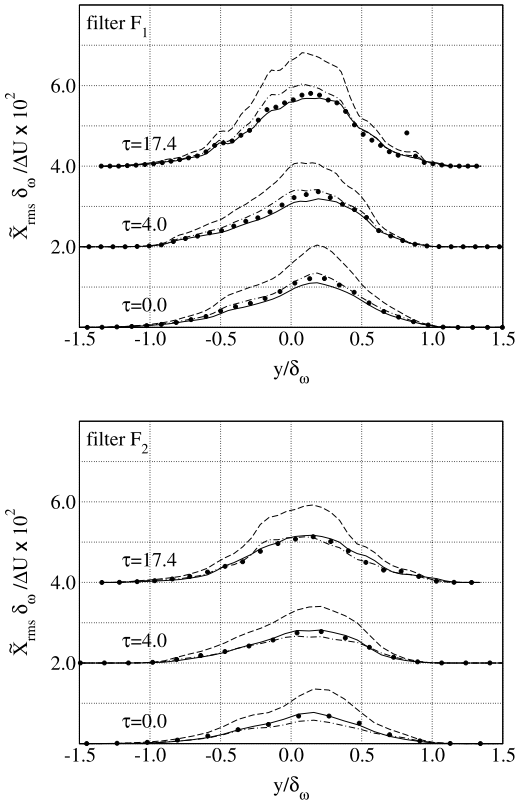


Fig. 3. Rms of the filtered scalar dissipation rate per unit mass: •, exact (filtered DNS); —, SSM model; - -, SMG model. Solid line indicates ARM model using Eq. (8). Times $\tau=4.0$ and $\tau=17.4$ have an offset in ordinates of 2.0 and 4.0, respectively.

and SMG, that was previously inaccurate for the subgrid dissipation, performs now very well. ARM predictions with Eq. (7) to model \tilde{X} (not shown), are similar to SSM ones. The fact that SMG performs inaccurately for $(X^{sg})_{rms}$ and accurately for \tilde{X}_{rms} indicates that model Eq. (7) is inappropriate: local equilibrium at the filter length scale, for the Reynolds number and α considered here, does not hold [18].

The use of Eq. (7) with a Smagorinsky model for q_Z has been also justified [7] as the first-order model proposed by Girimaji et al. [2], without appealing to a local equilibrium of the subgrid scales and without the intermediate field X^{sg} . According to the results presented here, this gradient-based approach describes better the spatial fluctuation, but the average value is excessively low. ARM can be used to alleviate this deficiency in the following way. The gradient model assumes

$$\bar{\rho} \tilde{X}^m = \rho D_Z \overline{|\nabla \tilde{Z}|^2} + \mu_T \overline{|\nabla \tilde{Z}|^2}, \quad (8)$$

if the cross term between resolved and unresolved scales is neglected and ρD_Z is constant. The first term in the right hand side of the equation above accounts for the resolved–resolved interactions, whereas the last term is the model for the contribution due to the unresolved scales. The coefficient μ_T , a turbulent diffusivity, has to be determined. Inserting Eq. (8) into Eq. (6) and neglecting the temporal change of subgrid scale variance, which has already been shown to be small, leads to the following equation for μ_T

$$(\rho D_Z + \mu_T) \int \langle \overline{|\nabla \tilde{Z}|^2} \rangle dy = \int \langle \bar{\rho} \rangle (\langle X^r \rangle^f + \langle X^{sg} \rangle^f) dy. \quad (9)$$

ARM, used for q_Z , provides better $\langle X^{sg} \rangle$ (see Fig. 1), and the derived coefficient μ_T (a constant for the whole field) leads consequently to a better prediction of $\langle \tilde{X} \rangle$ than with SMG or SSM. The behavior is similar to that shown in Fig. 1 and it is not repeated here. At the same time, ARM predictions of \tilde{X}_{rms} with this model, shown in Fig. 3, are as good as SMG ones. This approach is used in the ARM *a posteriori* case. However, it is noted that Eq. (8) neglects the cross term resolved-unresolved scales, which is not always small (from the DNS data, 15–25% of the total). Likewise, it would be interesting to see the behavior of this model for larger Reynolds numbers. Additional work is therefore still needed.

4.2. Filtered heat release

The second step consists in calculating the conditional filtered dissipation rate \tilde{X}_Z from \tilde{X} . Following normally practice [1], a one-dimensional mixing process is assumed by taking an instantaneous relation between \tilde{X} and Z derived from laminar solutions. Once \tilde{X}_Z is known, the heat release term is computed by Eq. (4). The subfilter variance needed in the filtered density function is calculated by ARM, its performance already reported to be very good for this type of non-linearity [12].

For small α , the behavior of \tilde{S} is similar to that of \tilde{X} , and SSM provides a 10% over-prediction. However, for large α , the algebraic value of the mean error $\langle \tilde{S}^m - \tilde{S} \rangle$ increases in comparison with $\langle \tilde{X}^m - \tilde{X} \rangle$. Thus, SMG leads to a 10–20% under-estimation, whereas that for \tilde{X} was 50%, SSM yields a 10–20% over-estimation, and ARM gives a 20–30% over-estimation. A similar behavior is observed in \tilde{S}_{rms} .

Therefore, SMG and SSM give errors in \tilde{X} comparable to those in \tilde{S} , and it is difficult to assess separately the accuracy of the models for \tilde{X}_Z . For instance, the compensation of errors shown by SMG would suggest that the laminar diffusion model is reasonably accurate, although

such a simplified description of the mixing process in this turbulent flow is questionable [11]. On the contrary, ARM predicts the field \tilde{X} better and errors in \tilde{S} due to the laminar mixing concept appear more clearly, showing the need of improvement of conditional dissipation models.

The mixing model proposed by Ref. [7], based on an average value of \tilde{X}_Z was also *a priori* tested within the ARM formulation. Results show a tendency to reduce the over-estimation of \tilde{S}_{rms} , but the over-estimation error in $\langle \tilde{S} \rangle^f$ grows at the same time, and it cannot be concluded that this statistical model is superior to the laminar mixing model.

5. *A posteriori* results

The non-dimensional governing LES equations, solved using Cartesian coordinates, are

$$\frac{\partial \rho}{\partial t} = -\frac{\partial(\rho u_k)}{\partial x_k}$$

$$\frac{\partial(\rho u_i)}{\partial t} = -\frac{\partial(\rho u_i u_k)}{\partial x_k} - \frac{\partial q_{u_i,ik}^m}{\partial x_k} + \frac{\partial \tau_{ik}}{\partial x_k} - \frac{\partial p}{\partial x_i}$$

$$\frac{\partial(\rho Z)}{\partial t} = -\frac{\partial(\rho Z u_k)}{\partial x_k} - \frac{\partial q_{Z,k}^m}{\partial x_k} + \frac{1}{ReSc} \frac{\partial}{\partial x_k} \left(\frac{\partial Z}{\partial x_k} \right)$$

$$\begin{aligned} \frac{\partial p}{\partial t} = & \frac{(\gamma - 1)Q}{(\gamma_0 - 1)M^2} \rho X_s^m P_s^m - \gamma P \frac{\partial u_k}{\partial x_k} \\ & - u_k \frac{\partial p}{\partial x_k} + \frac{\partial q_{p,k}^m}{\partial x_k} + (\gamma - 1)\Phi^m \\ & + \frac{\gamma/\gamma_0}{M^2 ReSc} T \left(\frac{W_0}{W_i} \frac{dY_i^e}{dZ} \right) \frac{\partial}{\partial x_k} \left(\frac{\partial Z}{\partial x_k} \right) \\ & + \frac{(\gamma - 1)/(\gamma_0 - 1)}{M^2 RePr} \frac{\partial}{\partial x_k} \left(\frac{C_p}{C_{p,0}} \frac{\partial T}{\partial x_k} \right) \\ & + \frac{(\gamma - 1)/(\gamma_0 - 1)}{M^2 ReSc} \left(\frac{C_{p,i}}{C_{p,0}} \frac{dY_i^e}{dZ} \right) \frac{\partial Z}{\partial x_k} \frac{\partial T}{\partial x_k}. \end{aligned}$$

The bar and tilde to indicate filtered quantities have been dropped and repeated subindices indicate summation. The superscript *m* indicates terms requiring closure; the viscous dissipation Φ is modeled like X and the remaining models have already been discussed. The main balance in the pressure equation (a form of energy equation), as observed from DNS, occurs between the heat release and the resolved dilatation terms appearing on the first line. The subgrid part of this dilatation term and of the three cross terms at the end of the energy equation have been found negligibly small. Taking as reference magnitudes the density of the outer streams, ρ_0 , the velocity difference ΔU , the initial vorticity thickness $\delta_{\omega,1}$, the temperature of the fuel stream $T_0 = 298$ K and the physical properties of oxygen W_0 and $C_{p,0}$, the

parameters are $Re = 8400$, $Pr = 0.7$, $Sc = 0.7$, $M = 0.69$ (convective Mach number 0.3) and $Q = Q_c/(C_{p,0} T_0) = 26.4$.

The initial condition for the LES is taken from the DNS filtered with F_2 at τ_1 . The mesh is $192 \times 122 \times 48$. The domain size is $19.7\delta_{\omega,1} \times 12.5\delta_{\omega,1} \times 4.2\delta_{\omega,1}$. The numerical algorithm is that of the DNS, i.e., a sixth-order compact scheme in space and a fourth-order Runge-Kutta in time, with non-reflective top and bottom boundary conditions [11].

Figure 4 shows three density contour plots. Only the central one-third of the computational domain is represented. The image on top is the filtered DNS at $\tau_1 = 0.0$, which is the initial condition for the LES. The two images on the bottom compare the filtered DNS with the LES performed with the ARM model at the final time $\tau_3 = 17.4$. Good qualitative prediction of the large scales provided by the LES is observed. Quantitatively, SMG and SSM yield a growth of the vorticity thickness smaller than the DNS one, and the vorticity thicknesses $\delta_{\omega}/\delta_{\omega,1}$ achieved at τ_3 are 1.44 and 1.48, respectively, while the filtered DNS value is $\delta_{\omega,3}/\delta_{\omega,1} = 1.69$. On the contrary, ARM provides a very accurate growth, 1.71.

Figure 5 shows the longitudinal spectrum of the resolved turbulent kinetic energy at τ_3 comparing filtered DNS with LES. First, it is seen that the energy content in the small resolved scales grows as the reconstruction level of the subgrid transport is increased. Second, the range of scales between non-dimensional wave-numbers 10 and 50 are significantly better predicted by ARM than by SMG or SSM. However, it is also observed that the smallest resolved scales, beyond non-dimensional wave-number of 50, depart from the filtered DNS data.

Figure 6 shows the mean and rms of the density field. The exact (DNS) value of $\delta_{\omega,3}$ has been

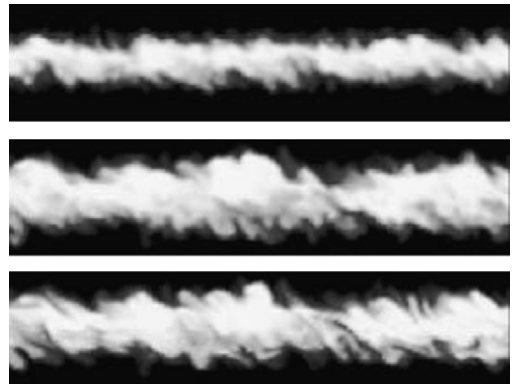


Fig. 4. Normalized density ρ/ρ_0 contour plots on a plane perpendicular to the spanwise homogeneous coordinate. White color indicates minimum values. Filtered DNS at $\tau = 0.0$ (top), filtered DNS at $\tau = 17.4$ (middle), LES using ARM at $\tau = 17.4$ (bottom).

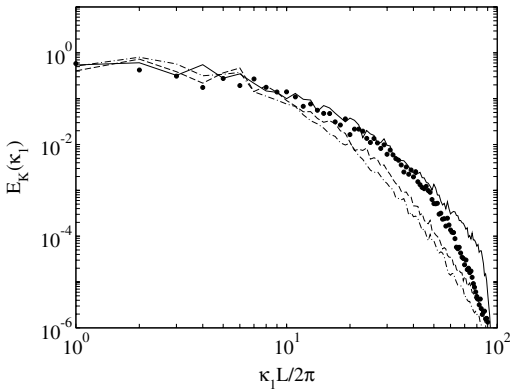


Fig. 5. One-dimensional turbulent kinetic energy spectra from LES at $\tau = 17.4$ and $y = 0$: \bullet , exact (filtered DNS); —, ARM model; --, SSM model; -·-, SMG model.

used to non-dimensionalize all the results. The mean density profile is in general well predicted, the accuracy increasing in the sequence SMG–SSM–ARM. This behavior can be related to the

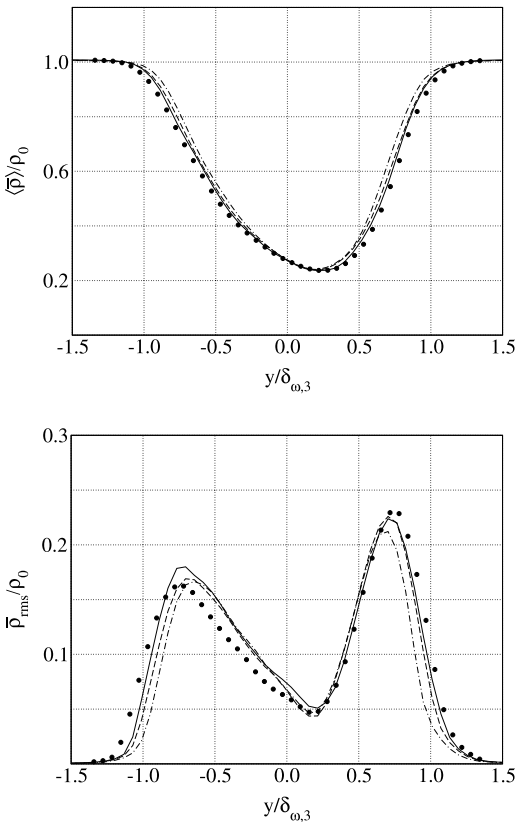


Fig. 6. Favre average (top) and turbulent fluctuation (bottom) of the density field from LES at $\tau = 17.4$: \bullet , exact (filtered DNS); —, ARM model; --, SSM model; -·-, SMG model.

prediction of the mean filtered heat release, shown in Fig. 7. The SMG and SSM under-predict $\langle \bar{S} \rangle^f$ and, consequently, the mean density is slightly over-predicted. Note however the strong difference between a priori and a posteriori model profiles given by SSM and, to a lesser degree, by SMG as well, the former over-estimating the heat release in the a priori context. On the contrary, ARM a priori results are maintained in the a posteriori case, showing a better overall prediction of $\langle \bar{S} \rangle^f$, which is consistent with a better $\langle \bar{\rho} \rangle$.

The correct prediction of $\bar{\rho}_{rms}$ is more complicated, as observed in Fig. 6. There is not only the fluctuation imposed by S_{rms} , shown in Fig. 7, but also the fluctuation imposed by the mixing with the outer cold fluid. In fact, this latter dominates, as deduced from the two strong peaks in $\bar{\rho}_{rms}$. Once again, there is an improvement in performance in the sequence SMG–SSM–ARM, particularly at the edges. However, there is a clear over-prediction in the interior side of the lower lobe, between $y / \delta_{\omega} = -1$ and the center line. This excess in $\bar{\rho}_{rms}$ is approximately the same with the three models, in spite of the differences in the prediction of S_{rms} .

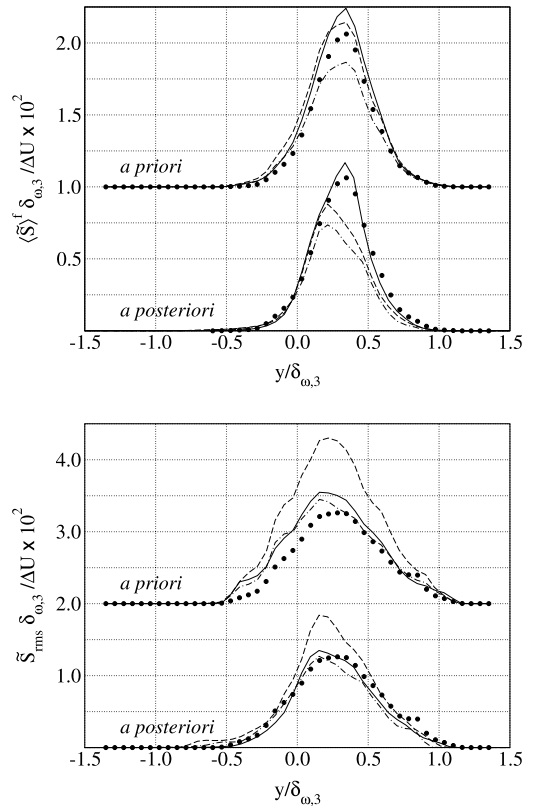


Fig. 7. Favre average (top) and turbulent fluctuation (bottom) of the filtered heat release per unit mass from LES at $\tau = 17.4$: \bullet , exact (filtered DNS); —, ARM model; --, SSM model; -·-, SMG model. Values normalized by $(\gamma_0 - 1)Q_c$.

6. Conclusion

Modeling of the filtered heat release term required for compressible LES of the turbulent infinitely fast reacting shear layer has been investigated, in particular the conditional filtered scalar dissipation rate at the stoichiometric surface, $\bar{\chi}_s$. This scalar dissipation rate is also required in subgrid closures based on flamelets or conditional moment closures in the case of flows with finite-rate chemistry. Results have indicated that a significant error is still present in the current available models, in large part from the modeling of the total filtered dissipation rate, $\bar{\chi}$.

Three subgrid transport models with an increasing sophistication in the reconstruction of the subgrid transport flux have been studied: dynamic Smagorinsky (SMG), dynamic mixed (SSM) and approximate reconstruction by moments with an additional Smagorinsky-type regularization term (ARM). *A priori* results have shown that the performance of the SMG and SSM models of the subgrid dissipation rate depends on the unresolved amount of turbulent fluctuation, whereas the ARM approach provides a filter-independent accurate prediction by using a minimum amount of physical information about the subfilter scales, namely, the integrated fluctuation energy.

It has also been observed that the model for $\bar{\chi}$ based on a local equilibrium hypothesis at the filter length-scales is not accurate. A gradient-based approach has been tested, using ARM to obtain the required model coefficient. This approach leads to better predictions of the mean and rms fluctuation of the filtered dissipation rate. However, the models for $\bar{\chi}_s$ require further improvement.

A posteriori results have shown an accurate prediction of the mean density and a reasonably good prediction of the rms density fluctuation. It has also been found that ARM provides a more realistic overall development of the shear layer, as observed in the thickness growth rate and the spectra.

The relative success in the LES results reported here and elsewhere is due to the small sensitivity of the considered turbulent reacting flows to the details of $\bar{\chi}_s$. However, extinction–reignition phenomena may demand more accurate models of micro-mixing. It has been shown that ARM resolves several

deficiencies of currently used models by providing a more accurate description of the subgrid energy transfer. Therefore, further development based on an ARM approach is a promising alternative.

Acknowledgment

The authors thank C. Pantano for the DNS data.

References

- [1] N. Peters, *Turbulent combustion*, Cambridge University Press, Cambridge, 2000.
- [2] S.S. Girimaji, Y. Zhou, *Phys. Fluids* 8 (5) (1996) 1224–1236.
- [3] J. Reveillon, L. Vervisch, *AIAA J.* 36 (3) (1998) 336–341.
- [4] A.W. Cook, W.K. Bushe, *Phys. Fluids* 11 (3) (1999) 746–748.
- [5] C.D. Pierce, P. Moin, *Phys. Fluids* 10 (1998) 3041–3044.
- [6] S.M. de Bruyn Kops, J.J. Riley, G. Kosály, *Flow Turbulence Combust.* 60 (1998) 105–112.
- [7] H. Pitsch, H. Steiner, *Proc. Combust. Inst.* 28 (2000) 41–49.
- [8] N. Branley, W.P. Jones, *Combust. Flame* 127 (2001) 1914–1934.
- [9] H. Forkel, J. Janicka, *Flow Turbulence Combust.* 65 (2000) 163–175.
- [10] S. Menon, W. Calhoun, *Proc. Combust. Inst.* 26 (1996) 59–66.
- [11] C. Pantano, S. Sarkar, F.A. Williams, *J. Fluid Mech.* 481 (2003) 291–328.
- [12] J.P. Mellado, S. Sarkar, C. Pantano, *Phys. Fluids* 15 (11) (2003) 3280–3307.
- [13] J. Bardina, J.H. Ferziger, W.C. Reynolds, *AIAA Paper* 80-1357, 1980.
- [14] S. Stolz, N.A. Adams, L. Kleiser, *Phys. Fluids* 13 (10) (2001) 2985–3001.
- [15] P. Moin, K. Squires, W. Cabot, S. Lee, *Phys. Fluids A* 3 (11) (1991) 2746–2757.
- [16] A.W. Vreman, *Phys. Fluids* 15 (8) (2003) L61–L64.
- [17] R.W. Bilger, in: P.A. Libby, F.A. Williams (Eds.), *Turbulent Reacting Flows*, Springer-Verlag, 1980, pp. 65–113.
- [18] C.B. da Silva, J.C.F. Pereira, *Phys. Fluids* 17 (10) (2005) 108103.

Comments

Dirk Roekaerts, Delft University of Technology, Netherlands. You showed that the profile of the filtered scalar dissipation rate, and in particular its maximal value, depends on the choice of filter. How can this be explained? Are there any simple general trends?

Reply. The mean profile of the filtered dissipation rate does not depend very much on the filter, but the partition

of the average filtered dissipation rate into the average resolved part and the average subgrid part does certainly depend for the large filters considered here. The resolved part is not negligible with respect to the subgrid part, and it decreases as the filter size increases because the smallest resolved scales remaining after the filter operation are larger and the corresponding gradients smaller. In turn, the subgrid dissipation rate increases (see Table 1).

On the other hand, the variance of the filtered dissipation rate diminishes as the filter becomes stronger, like for any other filtered field.



Forman Williams, University of California San Diego, USA. The ARM approach, as you have presented it, looks very good. Does it require appreciably more computation time than Smagorinsky?

Reply. Within the context of the dynamic formulation, the ARM approach requires more computational time than the Smagorinsky in the same way as the scale similarity model (dynamic mixed model) does. The main penalty is due to the dynamic closure of the Smagorinsky constant in all three cases, and the additional filter operation required by ARM in comparison with scale similarity is not so relevant.